Aus dem Institut für Physiologie
der Medizinischen Fakultät Charité – Universitätsmedizin Berlin

DISSERTATION

Time course of early microvascular collateral remodeling and neo-collateral formation after acute micro-occlusion in chick chorioallantoic membrane

zur Erlangung des akademischen Grades
Doctor of Philosophy (Ph.D.)

vorgelegt der Medizinischen Fakultät
Charité – Universitätsmedizin Berlin

Von

Weiwei Xiang
aus Hunan, China

Datum der Promotion: .....21.06.2020.....

Table of contents

List of Abbreviations

CAM	Chick chorioallantoic membrane
ECs	Endothelial cells
ECM	Extracellular matrix
VEGF	Vascular endothelial growth factor
Fps	Frame per second
IMG	Intussusceptive microvascular growth
MMPs	Matrix metalloproteinases
NE	Noradrenaline
NO	Nitric oxide
PBS	Phosphate-buffered saline
RBCs	Red blood cells
ROIs	Regions of interest
SD	Standard deviation
SE	Standard error of the mean
TG2	Transglutaminase 2
VSMCs	Vascular smooth muscle cells
WSS	Wall shear stress
Endothelial surface layer	ESL

Abstract

Arterial occlusive disease is the leading cause of morbidity and mortality throughout the developed world but current clinical treatment has yielded a less than satisfactory outcome. One reason for this limited success in treatment stems from a poor understanding of the process of vascular adaptation to a changing hemodynamic and metabolic environment. This mechanism underlies post-occlusive collateral formation including pre-existent collateral remodeling and neo-collateral formation.

It is an often stated concept that following arterial occlusion, pre-existent collaterals adapt to maintain the perfusion until initially elevated wall shear stress (WSS) normalizes. This concept, however, has not been corroborated by continuous observations of the morphological and hemodynamic changes in living vessels. In particular, the early phase of collateral adaptation, from the occurrence of occlusion to the beginning of cell proliferation in the vascular wall, is of critical clinical significance due to the limited time frame tissues undergoing ischemia can withstand. This early collateral remodeling, however, has been understood even less. In addition, existence of neo-collateral formation after acute arterial occlusion is still under debate.

Therefore this study aimed to determine by continuous microscopic observation the relationship between diameter of pre-existent collaterals and WSS during early adaptation and the occurrence of neo-collateral formation in the chick chorioallantoic membrane (CAM) after acute micro-occlusion.

To this end, a software was developed for repeated measurement of blood cell velocity in CAM (see publication III (P3) from Table of Contents). Three major issues concerning velocity measurement from *in vivo* videos were addressed including registration of video frames, segmentation of blood vessels and measurement of blood cell velocities. This software tool

was tested on CAM videos with various frame rates and was revealed to be a robust software in measuring blood velocities.

The structure and hemodynamics of CAM microvasculature were studied using intravital microscopy (see publication II (P2) from Table of Contents). On embryonic day 14 (E14), CAM microvasculature was observed to be arranged in an interdigitating fashion with a dense capillary mesh interconnecting the terminal and pre-terminal vessels. Our results revealed a proportionality of arteriolar velocity to vessel diameter and thus an approximate constancy of WSS throughout the arteriolar trees, suggesting adaptation of arteriolar diameters to WSS according to Murray's law. This finding based on direct hemodynamic measurements cannot be derived from simpler morphological assessments. The so called "junctional exponent" at divergent bifurcations was 2.05 ± 1.13 in contrast to 3 as predicted by Murray's law.

Early collateral remodeling and neo-collateral formation following acute micro-occlusion were then studied in CAM (see publication I (P1) from Table of Contents). Diameters of pre-existent collaterals exhibited an immediate decrease upon occlusion, then increased with a time constant of 2.5 ± 0.8 h and reached a plateau of up to 60% above baseline approximately 7 h post-occlusion. Vascular tone in the same vessels showed insignificant change through 24 h post-occlusion. Correspondingly, WSS exhibited an immediate increase upon occlusion and then decreased linearly to the baseline approximately 12 h post-occlusion.

WSS change and diameter change rate exhibited a two-phase reaction. The first phase featured an ever-expanding diameter with elevated WSS while in phase two, collateral diameter reached and persisted at a plateau level despite the sustained elevation of WSS. In addition, neo-collateral formation was observed by 23 h post-occlusion in the region adjacent to the occlusion site. Those newly formed collaterals might have developed from the capillary plexus in CAM.

In summary, CAM arteriolar collaterals undergo rapid collateral remodeling (<24 h) following acute occlusion. WSS might play a central role in regulating this process but other stimuli transferred from elsewhere in the CAM vascular network might also be contributing factors. Neo-collaterals form adjacent to the occlusion site within the same time frame and might have been created by the remodeling of pre-existent capillary meshes in CAM.

Zusammenfassung

Die arterielle Verschlusskrankheit ist eine der häufigsten Ursachen für Morbidität und Mortalität in den entwickelten Industrieländern. Ein wichtiger Grund für die limitierten Therapieansätze ist das geringe Verständnis der vaskulären Adaptation von Blutgefäßen an sich verändernde hämodynamische und metabolische Verhältnisse (postokklusive Kollateralbildung). Darunter zählen z.B. der Umbau bereits vorhandener Blutgefäße sowie die Neubildung von Kollateralen.

Ein gängiges Konzept der arteriellen Okklusion ist, dass prä- existierende Kollateralen adaptieren, um die Perfusion aufrechtzuhalten, solange sich die anfänglich erhöhte Wandschubspannung (WSS) normalisiert. Dieses Konzept wurde jedoch nicht durch kontinuierliche Beobachtungen der morphologischen und hämodynamischen Verhältnisse in lebenden Gefäßen bestätigt. Daher wurden bisher nur sehr begrenzte Kenntnisse über den zeitlichen Verlauf der kollateralen Gefäßantwort gewonnen. Insbesondere die frühe Phase der Kollateralbildung, vom Auftreten des Verschlusses bis zum Beginn der Zellproliferation in der Gefäßwand, ist von kritischer medizinischer Bedeutung. Darüber hinaus ist die Existenz einer Neokollaterale nach einem akuten arteriellen Verschluss noch umstritten.

Ziel dieser Studie ist es daher, den Zusammenhang zwischen dem Durchmesser einer vorbestehenden Kollateralen und der WSS während der frühen Phase der Adaptation nach akuter Mikrookklusion in der Chorioallantoismembran (CAM) befruchteter Hühnereier zu bestimmen. Hierfür wurde eine Software entwickelt um Geschwindigkeiten des Blutflusses in den Gefäßen der CAM zu bestimmen (Siehe Publikation III (P3) aus Inhaltsverzeichnis). Es wurden drei Hauptpunkte in Bezug auf die Geschwindigkeitsmessung adressiert: Registrierung der Videos, Segmentierung von Blutgefäßen und die Messung von Blutkörperchengeschwindigkeiten. Diese Software wurde an CAM-Videos mit verschiedenen Bildraten getestet und als robuste Software zur Messung von Blutgeschwindigkeiten etabliert.

Die Struktur und die Hämodynamik der CAM-Mikrovaskulatur wurden intravitalmikroskopisch untersucht (siehe Veröffentlichung II (P2) aus dem Inhaltsverzeichnis). Am Tag 14 (E14) der Embryonalentwicklung des Hühnereis würde das CAM-Mikrogefäßsystem in interdigitaler Weise angeordnet und mit einem dichten Kapillarnetz verbunden, welches die terminalen und prä-terminalen Gefäße miteinander verbindet. Die Ergebnisse zeigen ein proportionales Verhältnis der arteriellen Blutflussgeschwindigkeiten zum Gefäßdurchmesser. Damit einher geht eine konstante WSS entlang der arteriellen Gefäßbäume, was eine Anpassung der Arteriolendurchmesser an die WSS nach Murrays Gesetz nahelegt. Dieser Befund basiert auf direkten hämodynamischen Messungen und kann nur schwer von einfachen morphologischen Betrachtungen abgeleitet werden. Der sogenannte "Junctional Exponent" bei divergierenden Verzweigungen betrug 2,05 ± 1,13 im Gegensatz zu 3, wie nach Murrays Gesetz vorausgesagt.

Der frühe kollaterale Umbau und die Neokollateralbildung nach akuter Mikrookklusion wurden dann in der CAM untersucht (siehe Veröffentlichung I (P1) aus dem Inhaltsverzeichnis). Die Durchmesser der vorbestehenden Kollateralen verringerten sich unmittelbar nach dem Verschluss, stiegen dann mit einer Zeitkonstante von 2,5 ± 0,8 h an und erreichten etwa 7 h nach dem Verschluss ein Plateau von bis zu 60% über der Grundlinie. Hierbei veränderte sich der vaskuläre Tonus bis zu 24 h nach Okklusion nicht signifikant. Damit ging zunächst eine unmittelbare Zunahme WSS einher, welche dann linear bis ungefähr 12 Stunden nach der Okklusion wieder abnahm. WSS-Änderung und Durchmesseränderungsrate wiesen eine Zwei-Phasen-Verlauf auf. Phase I war gekennzeichnet durch einen ständig wachsenden Durchmesser mit erhöhter WSS, während in Phase II ein anhaltender Kollateral-Durchmesser mit über der Basislinie erhöhter WSS vorlag. Zusätzlich wurde die Bildung einer Neokollaterale 23 Stunden nach der Okklusion in einer zur Okklusionsstelle angrenzender Region beobachtet. Sie könnten sich aus dem Kapillarplexus der CAM entwickelt haben. Eine erhöhte WSS könnte ebenfalls der zugrundeliegende Stimulus für diesen Prozess sein.

Zusammenfassend findet in CAM-Kollateralen innerhalb von 24 Stunden nach der Okklusion ein schneller struktureller Umbau statt. Dieser Umbau könnte durch lokale WSS und andere Regulatoren innerhalb des mikrovaskulären Netzwerks vorangetrieben werden. Der zeitliche Verlauf zwischen der Bildung von Neo-Kollateralen und Umbauprozessen von Kollateralen ist ähnlich, der Stimulus für die Bildung von Neokollateralen in angrenzenden Regionen der Okklusionsstelle könnte ebenfalls die erhöhte WSS sein.

1 Introduction

1.1. Early collateral remodeling

Ischemia after acute arterial occlusion is the leading cause of morbidity and mortality across the developed world [1]. It requires medical attention as early after onset as possible because ischemic tissues, if left untreated, can progress quickly to infarction, leading to loss of function and threatening of life. Current pharmaceutical treatment (e.g., intravenous thrombolysis) and surgical intervention (e.g., mechanical thrombectomy), however, have yielded limited success in clinical outcomes. This discrepancy of outcome among patients has been associated largely with the various extents of available collateral flow [2], the blood flow established in the collaterals after occlusion. As one of the major determinants of prediction of infarct volume, collateral flow has emerged as the most important prognostic factor in acute arterial occlusive diseases [1].

Collateral flow upon occlusion (the baseline collateral flow), is dependent on collateral extent, the average diameter and number of pre-existent collaterals present in a tissue without obstructed flow [3]. Approximately 85% of the variation in collateral extent has been linked to a polymorphic genetic locus (Dce1) in mice [4]. Baseline collateral flow is clinically relevant in that it is an important determinant in the severity of tissue injury after arterial obstruction [5].

Collateral flow after arterial occlusion, on the other hand, is mainly determined by the process of collateral remodeling (arteriogenesis), an arteriogenic response of pre-existent arteriolar collaterals to the arteriolar occlusion. In human patients, the process of collateral remodeling can be negatively affected by several risk factors including diabetes mellitus, metabolic syndrome, hyperuricemia and aging [6]. Animal studies have revealed that collateral remodeling occurs in four stages. During the first phase (up to two days after occlusion), collateral endothelial cells (ECs) and vascular smooth muscle cells (VSMCs) transform into

proliferative and synthetic cells with increased vascular permeability. Stage two features focal digestion of the extracellular matrix and proliferations of ECs and VSMCs in the collateral wall. The third stage is characterized by rearrangement of SMCs into concentric layers, establishment of intercellular junctions among newly formed cells, and by synthesis of extra-cellular matrix. During stage four, some formed collaterals undergo pruning during adaptation [7] (Figure 1).

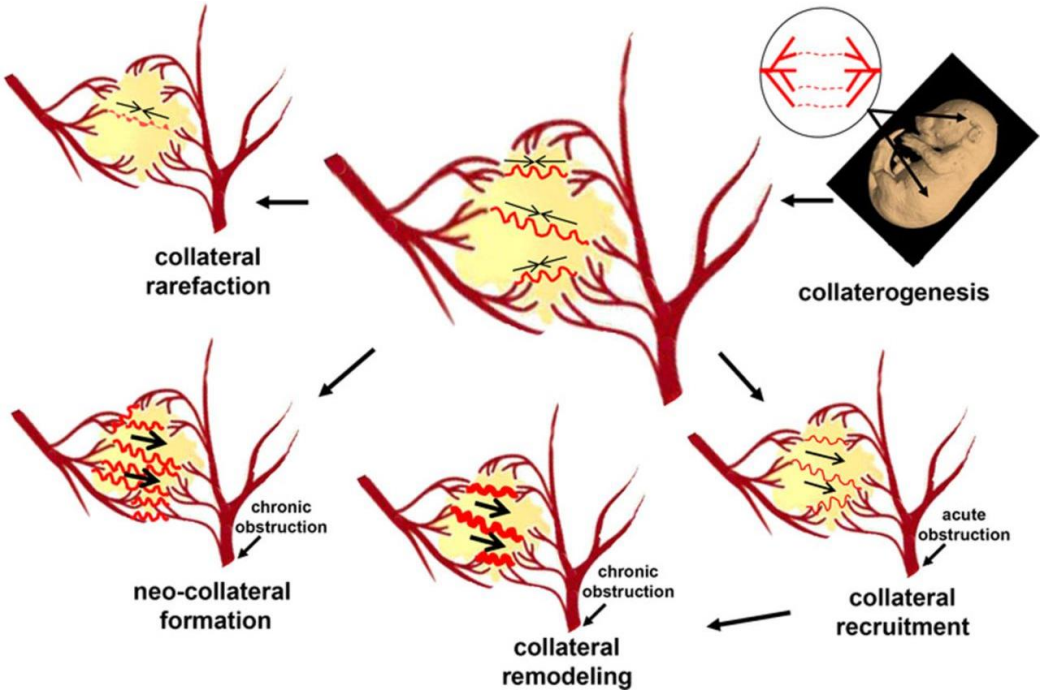

Figure 1. Lifecycles of collaterals in vascular networks. After acute obstruction, pre-existent arteriolar collaterals are recruited to undergo remodelling over time. In addition, neo-collaterals might develop to meet the needs of local metabolism [3].

Among the four stages of collateral adaptation, the first stage has been shown to be the most critical phase regarding salvaging the ischemic tissues. Re-establishment of perfusion by thrombolysis within two hours of occlusion can prevent infarction in about 50% of patients while thrombolysis between two and four hours only exhibits a higher chance of reducing infarction size rather than preventing infarction from occurring [8]. Despite their crucial clinical significance, details of early collateral adaptation, between the point of occlusion occurrence and the point of initial proliferation of vessel cells, has been scarcely reported.

1.2. Factors initiating and regulating collateral remodeling

Several stimuli, including WSS, blood pressure and ischemia, have been proposed to initiate and regulate collateral remodeling. WSS has been widely accepted as an initiator for collateral remodeling due to its skyrocketing in collaterals upon occlusion. WSS has also been proposed to drive collateral remodeling due to the observed simultaneity of WSS elevation and collateral enlargement [9,10]. The relationship between WSS and collateral remodeling during early collateral adaptation, however, has not been fully understood.

Blood pressure was once proposed as one of the stimuli initiating and driving collateral remodeling because it is the greatest mechanical force exerted by blood flow. It, however, decreases in the collateral upon occlusion due to the blood flow interruption, rendering it highly unlikely that blood pressure causes collateral diameter increase [7]. In addition, blood pressure can be outweighed by WSS over collateral growth. With blood pressure further lowered and blood flow further augmented by shunting the collateral flow directly into the veins, maximal collateral growth can be reached [11].

The simultaneous occurrence of ischemia and collateral remodeling after arterial occlusion renders it plausible to assume that ischemia might play a role in initiating collateral remodeling. This assumption has been further reinforced by the finding that ischemia can stimulate the transcription and translation of vascular endothelial growth factor (VEGF), a factor indispensable for collateral remodeling [12]. However, the long intermediate distance between the collateral and the downstream ischemic region indicates that ischemia might not be indispensable in promoting collateral remodeling [13]. Also, the well-oxygenated blood flowing through the enlarging collaterals in which VEGF is expressed, lessens the role of ischemia in collateral remodeling [7].

1.3. Neo-collateral formation

Neo-collateral formation is defined as *de novo* formation of “new” microvascular collaterals following arterial occlusion in adults [7] (Figure 1). It has been identified in human patients with moyamoya disease [14] in which collateral circulation establishes in pia mater that lacks capillaries under physiological conditions [15]. Thus far, two types of neo-collateral formation have been reported from experimental studies. The first type, observed in mouse skeletal muscles, is characterized by investment of mural cells to the wall of pre-existent capillary-like interconnections during the formation of neo-collaterals [16]. The other type, identified in the coronary [5] and cerebral microcirculation [17] of mice, emerges without pre-existent interconnecting vessels. The mechanisms underlying neo-collateral formation is not yet clear although ischemia has been proposed to play a role [17].

Neo-collateral formation can be of high clinical significance in that it provides a supplementary source of collateral circulation, given that a substantial segment of human population has poor pre-existent collaterals [3]. In addition, biological insight into neo-collateral formation may lead to identification of novel therapeutic targets in patients [5] as current pharmaceutical studies on arteriogenesis in animal models have yielded limited success in efficacy [18].

1.4. CAM and microvascular collateral remodeling

CAM is an extraembryonic membrane developing from the allantois and chorion membranes fusing together on embryonic day 3.5 (E3.5) [19]. CAM expands rapidly during embryo development generating a highly vascularized membrane that provides an interface for exchange of gas and waste [19]. As a relatively simple, quick, and economical model, CAM has been used as an *in vivo* model for a wide range of biomedical studies, e.g., angiogenesis [20,21], drug development [19] and tumor development [22]. The constant exposure of CAM to the ambient atmosphere, however, renders it a less suitable model for studies on the role of hypoxia in microvascular events. Thus far, use of CAM as a model in collateral studies has been very limited.

1.5. Aim of the study

The main goal of this study was to explore arteriolar collateral response within 24 hours of acute micro-occlusion. To this end, two minor questions and one major question were addressed in this study.

The two minor questions are as follows: (1) How can blood flow velocity, the critical determinant of WSS, be reliably obtained in CAM? Using *in vivo* videos of CAM, a robust software was developed, tackling three major issues of frame registration, vessel segmentation and velocity measurement. (2) How suitable a model is CAM in studying collateral response? By using intravital microscopy, the structure and hemodynamics of CAM microvasculature were quantitatively characterized.

The major question is: (3) What are the post-occlusive collateral responses within 24 hours of acute occlusion? Using intravital microscopy and the velocity software developed, collateral diameter and blood flow velocity were continuously recorded and computed. Emergence of neo-collaterals was continuously monitored during the same time window.

2 Materials and Methods

2.1 *Ex ovo* CAM model (P1, P2, P3)

Pathogen-free fertilized white leghorn chicken eggs (*domestic units*, VALO BioMedia GmbH, Cuxhaven, Germany) were placed horizontally in an incubator for embryonic development (BB16, Heraeus Instruments GmbH, Hanau, Germany) (temperature: 37.3°C; relative humidity: 70 - 80%). Sixty-five hours later, eggs were cracked open aseptically with a scalpel and the egg content was carefully transferred into a plastic tissue culture dish (internal diameter: 88mm (bottom), 100mm (top), TPP, Trasadingen, Switzerland). Chicken embryos were then placed back in the incubator and continued developing in the tissue culture dish until Hamburger-Hamilton stage 40 was reached on E14.

2.2 Intravital microscopy (P1, P2, P3)

On E14, chicken embryos were placed in a custom-made humidified chamber (T: 38°C) on the stage of the intravital microscope.

2.2.1 Single micro-occlusion in CAM microvasculature (P1)

Laser micro-beam (wavelength: 537 nm, effective spot diameter: approximately 24.3 µm, laser power: 100-170 mW, lasting period: 1 - 1.2 s) was employed to create single thrombus in CAM. Micro-occlusions were deemed successful if a single intravascular blood coagulum formed without damage to the vessel wall or to the surrounding tissue and without recanalization developing over the 24 hours that followed.

To pinpoint the microvascular collaterals of interest, an arteriolar collateral unit was defined as the first two orders of vessel segments from the two arteriolar trees that anastomose. This collateral unit includes four arteriolar segments: segment O_1, segment N_1, segment O_2, and segment N_2. Segment O_1, the first-order segment of the arteriolar tree occluded, and segment

N_1, the first-order segment of the arteriolar tree non-occluded, anastomose at a point at which two antegrade flows from each arteriolar tree meet. Segments O_2 and N_2 are the second-order segment neighbors of O_1 and N_1 respectively. The vessel segment occluded is the one immediately adjacent to segment O_2. To study neo-collateral formation, micro-occlusion was made on relative large arterioles (150 - 200 um) that were absent of anastomoses within three orders of segments downstream.

2.2.2 Continuous scanning of CAM microvascular collaterals (P1)

To study early collateral remodeling, collateral units were scanned using intravital microscopy at 15 time points spaced out over 24 hours: pre-occlusion (t = -1), upon occlusion (t = 0), every hour from one hour to 12 hours post-occlusion (t = 1,…,12) and 24 hours post-occlusion (t = 13). Images were taken with a CMOS-camera (Sony ICE 6000, Tokyo, Japan) and videos with a high speed camera (MotionBLITZ EoSens mini1-1, MC 1370, Mikrotron GmbH, Unterschleissheim, Germany). The objective used for both image and video acquisition was 10x, N.A. 0.22, (Leitz, Germany, trans-illumination). During the scanning interval, chicken embryos were placed back into the incubator to rest with optimal temperature and relative humidity.

To study neo-collateral formation, the occluded region was imaged (10x, N.A. 0.22, Leitz, Germany, trans-illumination) with a CMOS-camera (Sony ICE 6000, Tokyo, Japan) at four time points: pre-occlusion, upon occlusion, five hours post-occlusion and 23 hours post-occlusion. A zigzag-shaped scanning was adopted (six images for each row and six images for each column) with overlapping between adjacent images to enable photomontage.

2.2.3 Vascular tone *in vivo* (P1, P2)

A cocktail (75 µl) composed of acetycholine (100 µmol/L), adenosine (100 µmol/L), papaverine (200 µmol/L) and sodium nitroprusside (10 µmol/L) dissolved in PBS [23], was carefully

pipetted onto the collateral unit. The pipetted region was imaged (20x, N.A. 0.32, Leitz, Germany, trans-illumination) at pre-application of cocktail and 15 minutes post-application. Images were taken *in vivo* at three time points: pre-occlusion, three and 24 hours post-occlusion. Vascular tone was represented by the calculation:

$$VT = (D_{max} - D_{rest})/D_{max} \quad (1)$$

where VT is the vascular tone, D_{max} is the maximal diameter after dilation and D_{rest} indicates the resting diameter.

2.3 Offline measurements and calculations

2.3.1 Flow velocity measurement (P1, P2, P3)

Based on the principle of spatial correlation [24,25], a software tool was developed for the measurement of RBC velocity and was tested in CAM vascular networks (P3). The proposed software is composed of three modules, registration of video frames, segmentation of blood vessels and computation of RBC velocities. *Frame registration*. Irregular movements of blood vessels, caused by such factors as breathing of the animal, influence measurement of flow velocity; therefore, it is mandatory to remove them (movement correction) prior to velocity measurement. To this end, all frames from a given video were registered to the first frame for alignment. After the movement correction, a standard deviation image (SD image) was generated with intensity of each pixel corresponding to its SD from all frames. This SD image allows differentiation between static extravascular tissue (low SD value) and vessel lumen with flowing blood (higher SD value). *Vessel segmentation.* A semi-automatic approach to vessel segmentation was employed to acquire information on the position of a specific vessel segment. After a centerline of a vessel segment was traced manually as an initialization step, the software found the inner vessel wall automatically, thus having the vessels segmented. The original centerline was corrected corresponding to the newly computed vessel boundaries. *Centerline blood cell velocity measurement.* RBC aggregates and the intermediate plasma spacing exhibit a contrasted pattern when visualized under intravital microscope. This

microscopic pattern produces an intensity longitudinal file along the corrected centerline for each frame (P1, P3). Cross-correlation was then computed between consecutive profiles and the displacement was determined when the peak correlation value was achieved. Finally, on the correlation curve, three consecutive cardiac cycles shown to have characteristic pulsation were chosen for average velocity computation and the result was then given in average ± SD μm/s.

2.3.2 Calculation of average blood flow velocity, blood flow rate, wall shear stress and diameter change rate (P1, P2)

Blood velocity averaged across the lumen was calculated using the equation

$$V_b = V_c/1.6 \quad (2)$$

where V_b is the blood velocity averaged over the lumen, V_c is the centerline RBC velocity and 1.6 is the bluntness factor [26]. Blood flow was determined according to

$$Q = \pi D^2 V_b/4 \quad (3)$$

where Q is blood flow and D is luminal diameter. WSS was calculated as

$$\tau = 8\eta V_b/D \quad (4)$$

where τ is the WSS and the viscosity is

$$\eta = 1.3\ cP \quad (5)$$

Normalized diameter change rate, D_{norm}, between two adjacent time points t and $t+1$ was calculated as

$$D_{norm} = (\Delta D / \Delta T)/ \overline{D} \quad (6)$$

where D_t and D_{t+1} are the diameters for the two time points, diameter change as

$$\Delta D = D_{t+1} - D_t \quad (7)$$

and mean diameter as

$$\overline{D} = (D_{t+1} + D_t) / 2. \text{ with } \Delta T = 1 \text{ hour} \quad (8)$$

2.3.3 Time constant for diameter increase (P1)

During collateral enlargement, collateral diameters typically approached a plateau value by ten hours post-occlusion, with an approximately exponential increase relative to the baseline value. The diameters (*D*) were therefore fitted with a function of time:

$$D = a + b\,[1 - \exp(-t/t_c)] \tag{9}$$

where *a* and *b* are constants and t_c is the time constant of the diameter change.

2.3.4 Analysis of scaling properties (P2)

Scaling properties of CAM microvasculature were studied by analyzing the relationship of diameters (*D*) of vessels comprising a given bifurcation

$$D_0^{\,x} = D_1^{\,x} + D_2^{\,x} \tag{10}$$

where x indicates junctional exponent of the bifurcation studied. D_0 denotes the diameter of the parent vessel. D_1 and D_2 denote the diameters of the two daughter vessels respectively. According to Murray's law [27], the junctional exponent equals 3. In addition, the area ratio β and the symmetry ratio γ of bifurcations were calculated as follows:

$$\beta = (D_2^{\,2} + D_1^{\,2}) / D_0^{\,2} \tag{11}$$

$$\gamma = D_2 / D_1 \text{ with } D_2 \le D_1 \tag{12}$$

2.3.5 Functional capillary density (P1)

To estimate the changes in perfusion in the regions surrounding the occlusion site during collateral remodeling, functional capillary density, that is, the total length of perfusing capillary per CAM unit area, was measured in SD images (n = 5 CAMs) at four time points: pre-occlusion, upon occlusion, three hours post-occlusion and five hours post-occlusion. Four ROIs were delineated adjacent to each of the four collateral segments on each SD image (P1: Figure 2). The locations of the four ROIs remained unchanged through all four SD images for a given CAM. Area of ROI was calculated by multiplying the length by the width of the ROI. The total length of capillaries within each ROI was computed by virtue of the centerlines of the

capillary meshes manually drawn. Then the functional capillary density for each ROI was calculated as

$$dens_{cap} = L_{cap}/A_{ROI} \quad (13)$$

where $dens_{cap}$ denotes the functional capillary densities, L_{cap} is the total length of perfused capillaries within one ROI and A_{ROI} indicates the area of each ROI.

2.4 Electron microscopy (P2)

To visualize the CAM vascular network in greater detail, electron microscopy was performed according to Djonov et al. [28]. Freshly prepared Mercox solution (Vilene, Tokyo, Japan) containing 0.1 ml of accelerator/5 ml of resin was used to perfuse CAM. After the resin polymerized, CAMs were excised and transferred to 7.5% potassium hydroxide to dissolve the extravascular tissues that were underperfused. Next the corrosion casts were mounted on aluminum stabs and sputtered with 10 nm gold. The specimens with CAM vascular network were then studied with a Phillips scanning electron microscope (Philips XL 30) at various magnifications.

2.5 Statistical analysis (P1, P2)

All statistical analyses in this study were performed in SigmaPlot (Version 13, Systat Software Inc., San Jose, 237 California, USA). Sample size required for each experiment was determined using data from preliminary experiments in CAM (three CAMs for each preliminary experiment) with desired power of test set at 0.8. As a result, 13 CAMs were used for the study of the collateral adaptation from before occlusion up to 24 hours post-occlusion and 30 CAMs for vascular tone tests in collateral segments. Results are presented as mean ± SE (except otherwise stated). Means were compared using Student's *t*-test, paired *t*-test or repeated measures (RM) ANOVA followed by Student-Newman-Keuls test with equal or unequal variances as appropriate. Means were correlated using Pearson correlation. Differences were considered statistically significant at $P < 0.05$.

3 Results

3.1. Registration, segmentation and centerline blood cell velocity measurement by the software developed

Three modules were developed and tested in CAM videos: frame registration, vessel segmentation and velocity measurement. Compared with the noisy SD images yielded from the non-registered video frames, SD images from registered videos showed distinguishable boundaries of both capillaries and arterioles (P1: Figure 2; P3: Figure 2). Following the original manual tracing of centerlines, the semi-automatic approach segmented the vessels by finding the inner vessel limits automatically and then corrected the original centerline (P3: Figure 3). Along the corrected centerline of CAM vessels, patterns of intensity profile were acquired which was later used for displacement determination (P3: Figure 4).

Three frame rates (i.e., 25 fps, 50 fps and 200 fps) were tested (P3: Figure 6) to determine the optimal frame rate of video recording for velocity measurement in CAM vascular network. Videos of 25 fps exhibited least detail in intensity profile but were most memory-wise conservative. In contrast, videos of 200 fps gave a wealth of detail on intensity profile but were most memory-wise conservative. Videos of 50 fps were intermediate in performance and were eventually chosen for the final experiment (P3).

3.2. Structure and hemodynamics of CAM arteriolar trees without occlusion

3.2.1 Structure of arteriolar trees in CAM

At Hamburger-Hamilton stage 40, CAM microvasculature was arranged in an interdigitating fashion with a dense capillary mesh interconnecting the terminal and pre-terminal vessels (P1: Figure 2; P2: Figure 1, 7; P3: Figure 1). In arteriolar trees, diameters were 46.3 ± 39.2 μm and

declined along the blood flow direction (P2: Figure 2). Segment lengths of arterioles were [mean ± SD (median)]: D < 45 μm: 121 ± 66 μm (110 μm); 45 < D < 60 μm: 169 ± 88 μm (157 μm); 60 < D < 100 μm: 207 ± 169 μm (166 μm) (P2). In the absence of vascular occlusions, CAM microvascular networks developed pre-existent arteriolar collaterals (4.62 ± 1.44 collaterals / CAM, data unpublished).

Bifurcation parameters of arteriolar trees were shown in Table 1 (P2) including junctional exponent x, area ratio β, and symmetry ratio γ. In arteriolar trees, junctional exponent was 2.05 ± 1.1, substantially less than the value of 3 as predicted by Murray's law [27], which states that the energy cost for maintenance of the blood vessels and for transportation of blood flow is minimized if junctional exponent equals three. Mean area ratio and mean symmetry ratio were β = 0.94 ± 0.25 and γ = 0.53 ± 0.24 and both increased slightly as the parent vessel augmented in size (P2).

3.2.2 Hemodynamics of CAM arteriolar trees

In arteriolar trees, hemodynamic parameters of WSS, flow velocity and volume flow were quantitatively characterized and were all in accordance with Murray's law. WSS was [mean ± SD (median)] 4.47 ± 2.70 dyn/cm^2 (3.97 dyn/cm^2) and was approximately uniform throughout the arteriolar trees ($\tau \propto D^{1.03}$) (P2: Figure 3 and 8). Blood flow velocity increased almost proportionally to arteriolar diameter and the volume flow to the third power of arteriolar diameter (P1: Figure 3, Table 1; P2: Figure. 3 and 8).

3.3. Structural remodeling of pre-existent collaterals

3.3.1 Fast enlargement of pre-existent collateral was resultant of neither vascular growth nor vascular tone change

The occluded arterioles were 54.51 ± 10.78 μm (mean ± SD) in diameter. Collateral unit arterioles exhibited a fast enlargement after micro-occlusion with a mean time constant of 2.53

± 0.77 h (mean ± SD) for the four collateral segments studied. Specifically, diameters of the segment closest to the occlusion site exhibited an immediate decrease by 32% upon occlusion, progressively returned to baseline value three hours post-occlusion and remained at the baseline level through 24 hours post-occlusion. In contrast, the diameter change of the other three collateral unit segments exhibited a three-phase process, a significant decrease upon occlusion, an ensuing increase by up to 60% by four hours post-occlusion and then a plateau period until 24 hours post-occlusion (P1: Figure 4).

For each of the four segments in a collateral unit, diameters did not change significantly through 24 hours of development on E14 (paired *t*-test, n = 8 CAMs, $P > 0.05$) (P1: Figure S1). CAM arterioles exhibited a low resting vascular tone (≤10%) (P2), and so did the pre-existent resting arteriolar collaterals (P1: Figure S2). Compared with baseline values, vascular tone of the four segments did not change significantly three hours and 24 hours post-occlusion (ANCOVA, $P > 0.05$). No systematic trend in vascular tone change was observed among the four segments up to 24 hours post-occlusion (P1: Figure S2).

3.3.2 Collateral remodeling restored homogeneous distribution of wall shear stress and sequential decrease of diameter along the flow pathway

Before occlusion, WSS values showed no significant difference between any two of the four collateral unit segments, exhibiting a uniform WSS within the collateral unit. Upon occlusion, the homogeneity of WSS distribution was disturbed with an elevation to various extents for each segment. The uniformity of WSS distribution within the collateral unit was, however, restored by four hours post-occlusion to a similar level at which WSS was maintained pre-occlusion. This regained homogeneous WSS distribution persisted through to 24 hours post-occlusion (P1: Figure 3).

Before occlusion, collateral unit exhibited a bidirectional flow from the two converging arteriolar trees and diameters decreased significantly between neighboring arterioles in the direction of

blood flow. Immediately after occlusion, a unidirectional flow was established within the collateral unit and collateral diameter underwent adaptation in response to the blood flow disturbance. By four hours after occlusion, diameter decline along the blood flow was regained within the collateral unit and was sustained through to 24 hours post-occlusion (P1: Figure 3).

3.3.3 Collateral remodeling restored tissue perfusion surrounding the occlusion site

In the absence of occlusion, capillary meshes were ubiquitously formed in CAM to interconnect adjacent vessels and to perfuse surrounding tissues (P1: Figure 2; P2: Figure 1): Micro-occlusion, however, evoked changes in perfusion in the collateral unit region to meet metabolic demands. These perfusion changes were represented by the evolvement of the functional capillary mesh pattern (P1: Figure 2) and were evaluated with functional capillary density and with collateral blood flow in each segment (P1: Figure 2).

Upon occlusion, unidirectional flow was immediately established within the collateral unit. The CAM tissue adjacent to the occlusion site underwent ischemia following the lack of capillary flow. This capillary insufficiency was represented by the irregular dark area shown in the SD image (P1: Figure 2). Three hours post-occlusion, the under-perfused region shrank in size, suggesting an increase in capillary flow surrounding the occlusion site (P1: Figure 2). From five hours through to 24 hours post-occlusion, the under-perfused area was limited to the region immediately surrounding the occlusion site (P1: Figure 2).

Upon occlusion, functional capillary density adjacent to the segment closest to the occlusion site, underwent a decrease by approximately 50% compared with baseline level (ANOVA, $P < 0.05$), rebounded to 90% three hours post-occlusion (ANOVA, $P < 0.05$) and was completely restored five hours post-occlusion. Functional capillary densities adjacent to the other three segments showed no significant changes through five hours post-occlusion although a weak decline trend was observed upon occlusion (ANOVA, $P > 0.05$) (P1: Figure 2).

Blood flow in the segment closest to the occlusion site, decreased to approximately zero (ANOVA, $P < 0.05$) upon occlusion, recovered to baseline values three hours post-occlusion (ANOVA, $P < 0.05$) and remained unchanged through five hours post-occlusion (ANOVA, $P > 0.05$). Compared with baseline values, blood flow in the other three collateral unit segments did not change significantly upon occlusion, but increased significantly three hours post-occlusion (ANOVA, $P > 0.05$) and remained unchanged thereafter through to five hours post-occlusion (ANOVA, $P > 0.05$) (P1: Figure 2).

3.3.4 Wall shear stress might drive remodeling of pre-existent collaterals in CAM

Our results showed that WSS might be related to the fast collateral remodeling in CAM. The striking WSS elevation upon occlusion made a moderate contribution ($R^2 = 0.36$, $P < 0.05$) to the collateral diameter increase at one hour after occlusion and a milder contribution ($R^2 = 0.26$, $P < 0.05$) to the collateral enlargement at 24 hours post-occlusion (P1: Figure 7). In particular, the relationship between WSS and diameter change rate exhibited a two-phase process. In the first phase (up to seven hours post-occlusion), WSS elevated above baseline levels and diameter kept increasing. In phase two, WSS remained above baseline but diameters persisted after hitting the plateau level.

3.4. Neo-collaterals might arise from pre-existent capillary plexus

Neo-collateral formation following acute micro-occlusion was observed in this study. Before occlusion, no pre-existent collaterals were visualized within three orders of vessel segments downstream of the chosen occlusion site. By five hours after occlusion, collaterals were still yet to be identified in the region close to the occlusion site. By 23 hours post-occlusion, a neo-collateral had emerged three orders of vessel segments apart from the occlusion site. No pre-existent interconnections were observed before occlusion where the neo-collateral formed (P1: Figure 3).

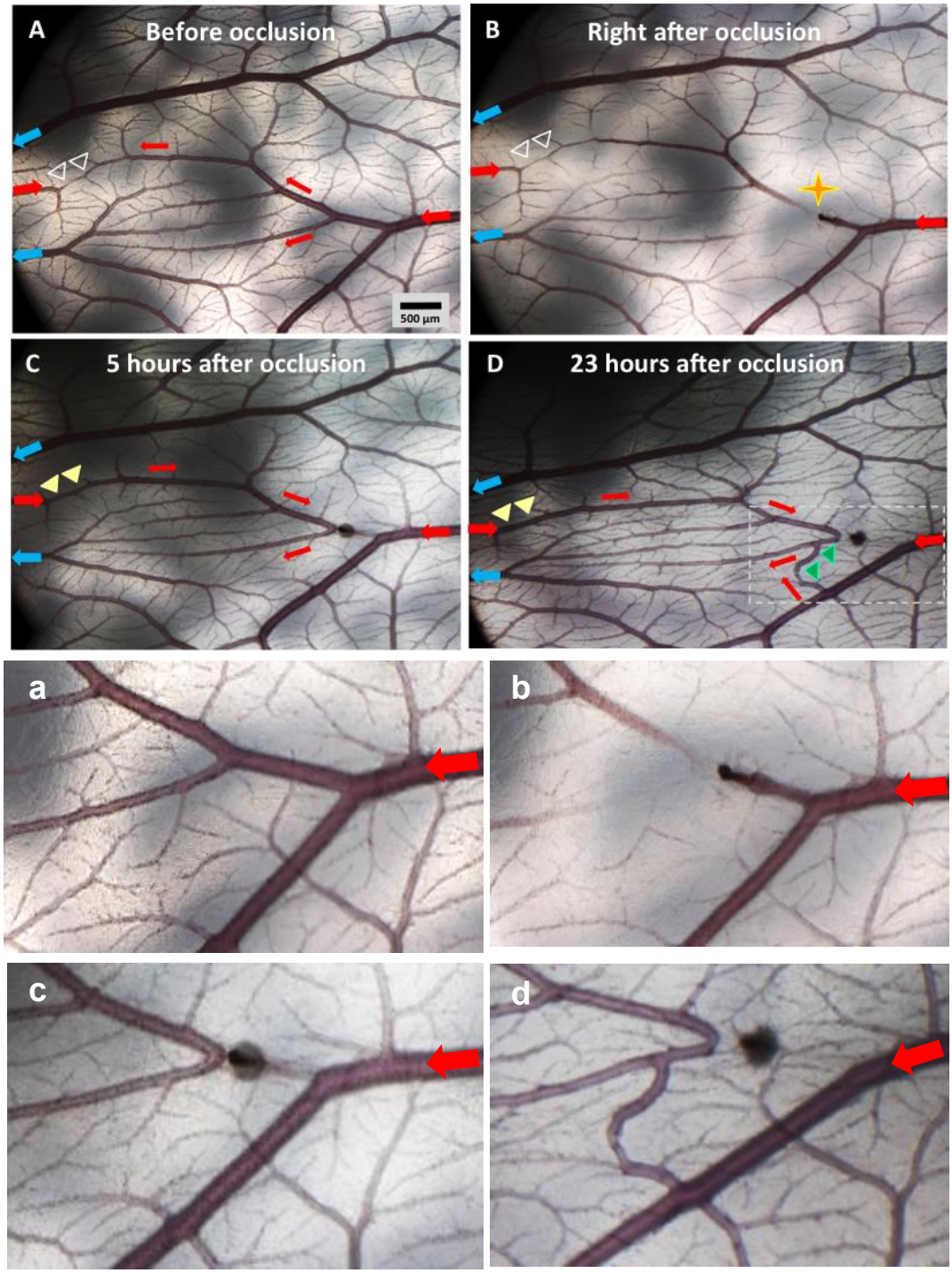

Figure 2. Neo-collateral formation within 24 hours of occlusion. Large red arrows: arterioles. Large blue arrows: venules. Small red arrows: flow direction. White arrowheads: pre-existing arteriolo-arteriolar anastomosis. Orange star: occlusion site. Yellow/green arrowheads: functional collaterals.

4 Discussion

We studied pre-existent collateral remodeling and neo-collateral formation in a CAM model within 24 hours after occlusion. In the absence of occlusion, the CAM microvascular network exhibited an interdigitating fashion with a dense interconnecting capillary network (P1, P2, P3). WSS was approximately constant throughout arteriolar trees in CAM, suggesting adaptation of arteriolar diameters in response to WSS (P2). Within 24 hours after acute micro-occlusion, pre-existent collaterals underwent fast structural remodeling with a time constant of 2.5 ± 0.8 hours (P1). This remodeling might be driven by local WSS elevation and by metabolic regulators travelling from elsewhere within the microvasculature (P1, P2). Neo-collaterals also formed in adjacent to the occlusion site possibly from the pre-existent capillary plexus (P1).

Given that RBCs move in the blood vessels at a speed proportional to flow velocity [25], RBC velocity was computed in our study as a measurement of flow velocity. In the software tool we developed, RBC velocities were computed along the vessel centerlines that were generated in SD images via a semi-automatic segmentation approach. This novel vessel segmentation approach yields a more realistic inner vessel limit and vessel centerline than a manual tracing (P1) and is in principle able to determine the displacement of RBC aggregates in a more realistic way. It is noteworthy though that the movement-dependent SD images might neglect the existence of the endothelial surface layer (ESL), thus underestimating the luminal diameter of blood vessels and returning the centerlines with deviations. ESL is a relatively static layer of membrane-bound glycocalyx that lies immediately atop the ECs [29]. Due to the fact that ESL ranges in thickness between several tens of nanometers determined by electron microscopy and 0.5 to over 1 µm measured *in vivo* [30], it is in principle plausible to accept the vessel boundaries and centerlines created by our software (P1, P2, P3). After obtaining the centerline blood cell velocity, an empirical factor of 1.6 was employed to convert the centerline RBC velocity to average blood velocity over the cross-sectional area of the vessel (P1, P2, P3)

because this bluntness factor of 1.6 holds true for a wide range of hematocrit and vessel size [31].

Another difficulty in determining RBC displacement lies in the possibility of tracked RBC aggregates changing patterns while moving in the vessel. Therefore, tracking single RBCs might be advantageous over tracking RBC aggregates in determining displacement between consecutive video frames. It is however, beyond the realms of possibility to track single RBCs in CAM arterioles due to the presence of multi-file flow rather than single file flow observed mainly in the smallest capillaries [30]. Therefore, our software tracks RBC aggregates and adopts a relative fast frame rate for video capturing (P1, P3) to limit the effect of RBC aggregate changing pattern between consecutive frames on displacement determination.

Our studies on the structure and hemodynamics of CAM vascular network (P1, P2) suggest that CAM is a suitable model to study collateral response. CAM has a collateral extent that is neither too high, thus forming a mesh of collaterals to hinder single collateral studies, nor too low for an appropriate collateral to be chosen (P1). Capillary mesh present in CAM (P1, P2) is reminiscent of the capillary source of neo-collaterals observed in other animal studies [16]. In the absence of occlusion, CAM arterioles exhibit diameter adaption in response to WSS (P1, P2), rendering CAM a good model to study the potential role of WSS in pre-existent collateral remodeling [7,9,10]. In addition, CAM microvascular network is readily exposed for experimentation (P2), making it possible to study its microvasculature continuously without disturbing its physiological status. The absence of innervation in CAM [32] renders hemodynamic and metabolic status the major factors regulating microvascular remodeling. Therefore, CAM provides a good model to study the collateral response of microvascular networks.

Intriguingly, although CAM arterioles are in line with a Murray-type optimization of hemodynamic parameters, they exhibit otherwise with their bifurcation parameters (e.g.,

junctional exponent) (P2). This morphological deviation from Murray's law might be associated with the finding that the small capillaries, along with the major large vessels (e.g., aorta), do not follow Murray's principle of optimization for minimal energy cost [33]. The other possibility of the bifurcation deviation from Murray's law concerns measurement errors which might exert a nonlinear effect on the relationship of the bifurcation parameters derived from the three arterioles comprising a given divergent bifurcation. The physiological significance of this deviation, however, seems to be low as evidenced by the finding that a large variation of the junctional exponent leads to only minor change in energy consumption (< 5%) [34]. Our bifurcation parameters, together with similar values gained from other tissues of different animals, might be more fitting with some alternative optimization principles, such as minimal use of wall material and optimal transport conditions [35,36].

Our studies show that collateral remodeling in CAM started within hours of occlusion which was much earlier (P1) than that in the mammalian models in which collateral remodeling did not initiate until several days after occlusion [7,9,10].This difference in the starting point of collateral remodeling likely concerns two aspects. First, WSS elevation might be more striking in our collateral unit than in mammalian models, leading to an early start of collateral remodeling in CAM. As opposed to CAM that has only one collateral pathway to bear all the increased flow that increases WSS, mammalian models often have multiple pre-existent collaterals in parallel that can be recruited upon occlusion [10]. This sharing of the increased blood flow by multiple parallel collaterals might lead to a less striking WSS elevation in individual collateral. Secondly, the starting point of collateral remodeling in mammalian models might be delayed with false negativity when collateral remodeling starts in capillaries rather than arterioles because capillaries and their early morphological changes could be too small for optical detection [16].

The cellular mechanisms underlying the fast collateral enlargement in CAM is not yet clear. It was not resultant of embryonic development (P1) or chronic reduction in vascular tone (P1).

Neither could it be the result of cellular proliferation because an estimate of 18 to 22 hours is needed for ECs and VSMCs to complete cell cycles during collateral enlargement [7]. One possibility of this fast collateral remodeling is the non-growth-related reorganization of vessel wall components, including VSMCs and extracellular matrix. During this reorganization, extracellular matrix is modified either in their structure, thus leading to morphological change, or in their turnover amount. VSMCs, on the other hand, can rearrange themselves by adjusting either their own lengths or by changing their overlapping lengths with nearby VSMCs, thus changing the vessel diameter [37]. For future experiments, digital reconstruction of collateral wall using multiphoton microscopy might be useful in revealing this VSMC rearrangement in CAM arteriolar network [37].

A significant correlation between WSS increase upon occlusion and diameter increase at two time points (i.e., one hour and 24 hours post-occlusion) was recorded (P1), indicating that WSS stimulates and promotes CAM collateral enlargement after acute micro-occlusion (P1), which is in agreement with others [9,10]. After micro-occlusion, collateral enlargement was preceded by WSS elevation (P1).and continued while WSS was above the baseline value during the first seven hours post-occlusion (P1). Nitric oxide (NO), an endothelial product following WSS elevation, might play a role in mediating the rapid collateral remodeling in CAM but further experiments are needed to test this hypothesis. In particular, pharmaceutical experiments (e.g., inhibition of endothelium by N (gamma)-nitro-L-arginine methyl ester) and/or genetic animal models (e.g., endothelial NO synthase knockout mice) might be helpful in this regard [7].

Interestingly, WSS was still above baseline values while collateral diameters remained unchanged in the second phase of adaptation (from seven hours post-occlusion onwards) (P1: Figure 4). This is incongruent with the commonly accepted concept that elevated WSS drives collateral enlargement until WSS returns to baseline values [10,38]. One possibility for this mismatch concerns the anatomic limits for collateral growth set by the collateral wall

composition and by the interaction between collaterals and WSS exerted on the collateral wall. Once the collateral enlargement reaches a certain level, it ceases unless anatomic components change (e.g., cellular proliferation) or stronger stimuli (e.g., stronger WSS elevation produced by arterio-venous fistula) emerge [39]. In our CAM model, with proliferation of ECs and VSMCs yet to start, collaterals might have reached the maximum diameter its anatomic composition allows for and thus were incapable for further growth despite persistent elevated WSS. The other possible explanation for this mismatch is that structural adaptation of collateral diameters depends not only on local WSS but also on other biological stimuli including signals propagating along vessel walls from the adjacent vessels [40]. Thus, the observed WSS changes may reflect not only local hemodynamic conditions but also flow resistance and local conditions elsewhere in the microvascular network. The continued decline in WSS while diameter stabilized suggests that vessels elsewhere in the network undergo slower adaptation. Within this framework, stable vessel diameters could result from a decreasing WSS stimulus balanced by other increasing stimuli, e.g. local metabolic signals or conducted responses [7]. To study information transfer of metabolic status between collateral unit and surrounding vascular network in CAM, connexin studies in the collateral wall, via immunohistostaining or western blot, could be helpful given that conducted responses are mediated by gap junctions composed of connexins [40].

Sprouting angiogenesis was not considered in the present study given the short timeline covered and given that ischemia, a potent stimulus for sprouting angiogenesis, is not likely to occur in CAM model with its constant exposure to the ambient atmosphere. However, our study suggests that intussusceptive microvascular growth (IMG), the other type of angiogenesis, might play a role in the fast recovery of perfusion in the regions downstream of micro-occlusion (P1). Under physiological conditions, IMG contributes to the development of microvascular network in CAM from E7 to E14 [21], allowing microvascular growth and remodeling with an extremely low proliferation rate of ECs [20]. With increased blood flow,

however, IMG can occur within one hour [20] which fits the time frame of the recovery of capillary densities observed in CAM (P1).

In summary, on E14, CAM microvasculature exhibited an interdigitating arrangement with a dense capillary plexus interconnecting adjacent vessels. Wall shear stress in CAM arterioles was approximately uniform, indicating arteriolar diameter adaptation to wall shear stress. After an acute micro-occlusion, CAM collaterals underwent structural remodeling within 24 hours of occlusion and WSS might play a critical role in this process. Neo-collaterals emerged in CAM by 24 hours post-occlusion, likely from pre-existent capillary plexus.

References

1. de Marchi SF, Gloekler S, Meier P, Traupe T, Steck H, Cook S, Vogel R, Seiler C. Determinants of preformed collateral vessels in the human heart without coronary artery disease. *Cardiology*. 2011;118:198-206.

2. Leng X, Lan L, Liu L, Leung TW, Wong KS. Good collateral circulation predicts favorable outcomes in intravenous thrombolysis: a systematic review and meta-analysis. *Eur J Neurol*. 2016;23:1738-1749.

3. Faber JE, Chilian WM, Deindl E, van Royen N, Simons M. A brief etymology of the collateral circulation. *Arterioscler Thromb Vasc Biol.* 2014;34:1854-1859.

4. Sealock R, Zhang H, Lucitti JL, Moore SM, Faber JE. Congenic fine-mapping identifies a major causal locus for variation in the native collateral circulation and ischemic injury in brain and lower extremity. *Circ. Res.* 2014;114:660-671.

5. Zhang H, Faber JE. *De-novo* collateral formation following acute myocardial infarction: Dependence on $CCR2^{+}$ bone marrow cells. *J Mol Cell Cardiol.* 2015;87:4-16.

6. Menon BK, Smith EE, Coutts SB, Welsh DG, Faber JE, Goyal M, Hill MD, Demchuk AM, Damani Z, Cho KH, Chang HW, Hong JH, Sohn SI. Leptomeningeal collaterals are associated with modifiable metabolic risk factors. *Ann Neurol.* 2013;74:241-248.

7. Schaper W. Collateral circulation, Past and present. *Basic Res Cardiol.* 2009;104:5-21.

8. Davies GJ, Chierchia S, Maseri A: Prevention of myocardial infaretion by very early intracoronry streptokinase: relative role of thrombosis and spasm. *N Engl J Med.* 1984;311:148

9. Gruionu G, Hoying JB, Pries AR, Secomb TW. Structural remodeling of the mouse gracilis artery: coordinated changes in diameter and medial area maintain circumferential stress. *Microcirculation*. 2012;19:610-618.

10. Unthank JL, Fath SW, Burkhart HM, Miller SC, Dalsing MC. Wall remodeling during luminal expansion of mesenteric arterial collaterals in the rat. *Circ Res.* 1996;79:1015-1023.

11. Eitenmüller I, Volger O, Kluge A, Troidl K, Barancik M, Cai WJ, Heil M, Pipp F, Fischer S, Horrevoets AJ, Schmitz-Rixen T, Schaper W. The range of adaptation by collateral vessels after femoral artery occlusion. *Circ Res.* 2006;99:656-662.

12. Matsunaga T, Warltier DC, Weihrauch DW, Moniz M, Tessmer J, Chilian WM. Ischemia-induced coronary collateral growth is dependent on vascular endothelial growth factor and nitric oxide. *Circulation.* 2000;102:3098-3103.

13. Wagner S, Helisch A, Ziegelhoeffer T, Bachmann G, Schaper W. Magnetic resonance angiography of collateral vessels in a murine femoral artery ligation model. *NMR Biomed.* 2004;17:21-27.

14. Smith ER, Scott RM. Spontaneous occlusion of the circle of Willis in children: pediatric moyamoya summary with proposed evidence-based practice guidelines. A review. *J Neurosurg Pediatr*. 2012;9:353-360.

15. Duvernoy HM. Vascularization of the cerebral cortex. *Rev Neurol (Paris)*. 1999;155:684-6 87.

16. Mac Gabhann F, Peirce MS. Collateral Capillary Arterialization following arteriolar ligation in murine skeletal muscle. *Microcirculation.* 2010;17:333-347.

17. Zhang H, Prabhakar P, Sealock R, Faber JE. Wide genetic variation in the native pial collateral circulation is a major determinant of variation in severity of stroke. *J Cereb Blood Flow Metab*. 2010;30:923-934.

18. Rubanyi GM. Mechanistic, technical, and clinical perspectives in therapeutic stimulation of coronary collateral development by angiogenic growth factors. *Mol. Ther*. 2013;21:725-738.

19. Ribatti D. The chick embryo chorioallantoic membrane (CAM). A multifaceted experimental model. *Mech Dev.* 2016;141:70-77.

20. Djonov V, Baum O, Burri PH. Vascular remodeling by intussusceptive angiogenesis. *Cell Tissue Res.* 2003;314:107-117.

21. Djonov VG, Galli AB, Burri PH. Intussusceptive arborization contributes to vascular tree formation in the chick chorioallantoic membrane. *Anat Embryol (Berl).* 2000;202:347-357.

22. Dagg CP, Karnofsky DA, Roddy J. Growth of transplantable human tumors in the chick embryo and hatched chick. *Cancer Res*. 1956;16:589-594.

23. Werner J. Contribution of endothelial autacoids to the regulation of arteriolar tone in skeletal muscle in vivo. [Dissertation]. July 9,2001. http://www.diss.fu-berlin.de/2001/115/index.html. Accessed November 12, 2016.

24. Pries AR, Secomb TW, Gaehtgens P. Design principles of vascular beds. *Circ Res*. 1995; 77:1017-1023.

25. Pries AR, A versatile video image analysis system for microcirculatory research. *Int J Microcirc Clin Exp.* 1988;7:327-345.

26. Pittman RN, Ellsworth ML. Estimation of red cell flow microvessels: consequences of the Baker-Wayland spatial averaging model. *Microvasc Res.* 1986;32:371-388.

27. Murray CD. The physiological principle of minimum work: i. the vascular system and the cost of blood volume. *Proc Natl Acad Sci.* 1926;12:207-214.

28. Djonov VG, Kurz H, Burri PH. Optimality in the developing vascular system: Branching remodeling by means of intussusception as an efficient adaptation mechanism. *Dev Dyn*. 2002;224:391-402.

29. Pries AR, Secomb TW, Gaehtgens P. The endothelial surface layer. *Pflugers Arch.* 2000;440:653-666.

30. Pries AR, Secomb TW. Rheology of the microcirculation. *Clin Hemorheol Microcirc.* 2003;29:143-148.

31. Baker M, Wayland H. On-line volume flow rate and velocity profile measurement for blood in microvessels. *Microvasc Res.* 1974;7:131-143.

32. Regan T. *Animal Sacrifices. Animal sacrifices, Religious perspectives on the use of animals in science.* Temple University Press, 1987.

33. Sherman TF. On connecting large vessels to small. The meaning of Murray's law. *J Gen Physiol.* 1981,78:431-453.

34. Sherman TF, Popel AS, Koller A, Johnson PC. The cost of departure from optimal radii in microvascular networks. *J Theor Biol.* 1989;36:245-265**.**

35. Kurz H, Sandau K. Modeling of blood vessel development: bifurcation pattern and hemodynamics, optimality and allometry. *Comments on Theor Biol.* 1997;4:261-291.

36. West GB, Brown JH, Enquist BJ. A general model for the origin of allometric scaling laws in biology. *Science.* 1997;276:122-126.

37. Martinez-Lemus LA, Hill MA, Bolz SS, Pohl U, Meininger GA. Acute mechanoadaptation of vascular smooth muscle cells in response to continuous arteriolar vasoconstriction: implications for functional remodeling. *FASEB J.* 2004;18:708-710.

38. Buschmann I, Pries A, Styp-Rekowska B, Hillmeister P, Loufrani L, Henrion D, Shi Y, Duelsner A, Hoefer I, Gatzke N, Wang H, Lehmann K, Ulm L, Ritter Z, Hauff P, Hlushchuk R, Djonov V, van Veen T, le Noble F. Pulsatile shear and Gja5 modulate arterial identity and remodeling events during flow-driven arteriogenesis. *Development.* 2010;137:2187-2196.

39. Pipp F, Boehm S, Cai WJ, Adili F, Ziegler B, Karanovic G, Ritter R, Balzer J, Scheler C, Schaper W, Schmitz-Rixen T. Elevated fluid shear stress enhances postocclusive collateral artery growth and gene expression in the pig hind limb. *Arterioscler Thromb Vasc Biol.* 2004;24:1664-1668.

40.Pries AR, Reglin B, Secomb TW. Structural adaptation of microvascular networks: functional roles of adaptive responses. *Am J Physiol Heart Circ Physiol.* 2001;281:H1015-H10

Affidavit

I, Weiwei Xiang, certify under penalty of perjury by my own signature that I have submitted the thesis on the topic "*Time course of early microvascular collateral remodeling and neo-collateral formation after acute micro-occlusion in chick chorioallantoic membrane*". I wrote this thesis independently and without assistance from third parties, I used no other aids than the listed sources and resources.

All points based literally or in spirit on publications or presentations of other authors are, as such, in proper citations (see "uniform requirements for manuscripts (URM)" the ICMJE www.icmje.org) indicated. The sections on methodology (in particular practical work, laboratory requirements, statistical processing) and results (in particular images, graphics and tables) correspond to the URM (s.o) and are answered by me. My contributions in the selected publications for this dissertation correspond to those that are specified in the following joint declaration with the responsible person and supervisor. All publications resulting from this thesis and which I am author of correspond to the URM (see above) and I am solely responsible.

The importance of this affidavit and the criminal consequences of a false affidavit (section 156,161 of the Criminal Code) are known to me and I understand the rights and responsibilities stated therein.

---------- ----------

Date, location Signature

Declaration of personal contributions to co-authored publications

Weiwei Xiang had the following share in the following publications:

Publication I: Xiang W, Reglin B, Rong W, Nitzsche B, Maibier M, Hoffmann B, Ruggeri A, Guimarães P, Secomb TW and Pries AR. Hemodynamic remodeling of arteriolar collaterals after acute occlusion in chick chorioallantoic membrane. *Microcirculation*. 2017,24(4).
Impact Factor: 2.797

Contribution in detail: Central participation in the development of concepts, design of experiments, selection of methodologies, conducting of animal experiments, analysis of data collected and composition of manuscript.

Publication II: Maibier M, Reglin B, Nitzsche B, **Xiang W,** Rong W, Hoffmann B, Djonov V, Secomb TW and Pries AR. Structure and function of vascular networks in the chorioallantoic membrane of the chicken. *Am J Physiol Heart Circ Physiol.* 2016,311(4):H913-H926.
Impact Factor: 3.569

Contribution in detail: Participation in the image acquisition of two CAM microvascular networks using intravital microscopy and in the reconstruction and analysis of those images.

Publication III: Guimarães P, **Xiang W**, Wigdahl J, Reglin B, Pries A and Ruggeri A. Measuring blood flow velocity from intravital video recordings. *Conf Proc IEEE Eng Med Biol Soc.* 2015,6289-6292.
Impact Factor: 0.76

Contribution in detail: Participation in the design of the study, experimentation in CAM and in the development and testing of the software.

Signature, date and stamp of the supervising University teacher

_____

Signature of the doctoral candidate

_____

Publication I:

Xiang W, Reglin B, Rong W, Nitzsche B, Maibier M, Hoffmann B, Ruggeri A, Guimarães P, Secomb TW and Pries AR. Hemodynamic remodeling of arteriolar collaterals after acute occlusion in chick chorioallantoic membrane. *Microcirculation*. 2017,24(4).

DOI: http://dx.doi.org/10.1111/micc.12351

Publication II:

Maibier M, Reglin B, Nitzsche B, **Xiang W,** Rong W, Hoffmann B, Djonov V, Secomb TW and Pries AR. Structure and function of vascular networks in the chorioallantoic membrane of the chicken. *Am J Physiol Heart Circ Physiol.* 2016,311(4):H913-H926.

DOI: http://dx.doi.org/10.1152/ajpheart.00786.2015

Publication III:

Guimarães P, **Xiang W**, Wigdahl J, Reglin B, Pries A and Ruggeri A. Measuring blood flow velocity from intravital video recordings. *Conf Proc IEEE Eng Med Biol Soc.* 2015,6289-6292.

DOI: http://dx.doi.org/10.1109/EMBC.2015.7319830

Curriculum Vitae

For reasons of data protection law, my CV is not published in the electronic version of my work.

Complete list of publications

1. Guimarães P, **Xiang W**, Wigdahl J, Reglin B, Pries A and Ruggeri A. Measuring blood flow velocity from intravital video recordings. *Conf Proc IEEE Eng Med Biol Soc.* 2015,6289-6292.

2. Maibier M, Reglin B, Nitzsche B, **Xiang W,** Rong W, Hoffmann B, Djonov V, Secomb TW and Pries AR. Structure and function of vascular networks in the chorioallantoic membrane of the chicken. *Am J Physiol Heart Circ Physiol.* 2016,311(4):H913-H926.

3. **Xiang W**, Reglin B, Rong W, Nitzsche B, Maibier M, Hoffmann B, Ruggeri A, Guimarães P, Secomb TW and Pries AR. Hemodynamic remodeling of arteriolar collaterals after acute occlusion in chick chorioallantoic membrane. *Microcirculation.* 2017,24(4).

Poster Presentations

1. Xiang W, Reglin B, Rong W, Nitzsche B, Maibier M, Ruggeri A, Guimarães P, Secomb TW, Pries AR, Dynamic remodeling of arteriolar collaterals after acute occlusion in chick chorioallantoic membrane. Frontiers in CardioVascular Biology, Florence, July 2016.

2. Rong WW, Reglin B, **Xiang W**, Nitzsche B, Maibier M, Pries AR. “Emerging angiogenesis” in the chick chorioallantoic membrane. An *in vivo* study. Frontiers in CardioVascular Biology, Florence, July 2016.

3. **Xiang W**, Reglin B, Rong W, Nitzsche B, Maibier M, Ruggeri A, Guimarães P, Secomb TW, Pries AR. Early adaptation of pre-existing arteriolar collateral after acute microocclusion: an *in vivo* study in chick chorioallantoic membrane. Experimental Biology, San Diego, April 2016.

4. **Xiang W**, Reglin B, Rong W, Nitzsche B, Maibier M, Ruggeri A, Guimarães P, Secomb TW, Pries AR. Neo-collateral formation supplements collateral remodelling after acute arteriolar occlusion in the chick chorioallantoic membrane. 10th World Congress for Microcirculation, Kyoto, September 2015.

5. **Xiang W**, Reglin B, Rong W, Nitzsche B, Maibier M, Ruggeri A, Guimarães P, Secomb TW, Pries AR. Vascular Collateralization Investigated in the Chorio-Allantoic Membrane (CAM). Summer school of European Society of Cardiology. Nice, France, June, 2015.

6. **Xiang W**, Reglin B, Rong W, Nitzsche B, Maibier M, Ruggeri A, Guimarães P, Secomb TW, Pries AR. Vascular Collateralization Investigated in the Chorio-Allantoic Membrane (CAM). Experimental Biology, Boston, April 2015.

7. **Xiang W**, Reglin B, Nitzsche B, Maibier M, Sehmsdorf T, Pries AR. Vascular reactions to local occlusion: collateralization and structural adaptation. A chorioallantoic membrane study. The 3rd Joint Meeting of the German Society for Microcirculation and Vascular Biology (GfMVB) and the Swiss Society for Microcirculation and Vascular Research (SSMVR) and the 36th Annual Meeting of the GfMVB. Muenster, Germany. September, 2014.

8. Maibier M, Nitzsche B, Reglin B, **Xiang W**, Secomb TW, Höpfner M, Pries AR. Structure and hemodynamics in the chick chorioallantoic membrane: Murray's law revisited. Frontiers in CardioVascular Biology, Barcelona, July 2014.

Acknowledgements

I am deeply indebted to my Ph.D. supervisor, Herr Prof. Dr. med. Axel Radlach Pries, the current Dean of Charité - Universitätsmedizin Berlin, who, I believe, is a great epitome of enthusiasm, perseverance and dedication to science. Not only did he impart to me the importance of thoroughness and detail-focus in science, he also made the beauty of integrating science and art visible to me guiding me through my wonderful Ph.D. journey. I am also greatly obliged to Dr. Bettina Reglin for the countless beautiful scientific discussions, for her support of my career goals and for her sparing time to help me pursue those goals. Many thanks to Dr. rer. nat. Bianca Nitzsche, Prof. Dr. Wolfgang Kuebler, Dr. med. Martin Maibier, Dr. Pedro Guimarães and Prof. Dr. Timothy Secomb for the wonderful exchange of ideas on my project and for their insightful input to the manuscript. I would also like to thank Björn Hoffmann for his constant help with tough technical problems encountered during my experiment. Special thanks go to Dr. med. Andreas Zakrzewicz and Prof. Dr. med. Helmut Habazettl for their valuable opinions on the experimental design and statistical analysis respectively. I would also like to express my gratitude to Wenwei Rong, Dr. rer. nat. Janine Berkholz, Laura Michalick, Weronika Kuzyniak, Gustav Steinemann, Sylvia Plog and Angela Becker from the Institute of Physiology for the cordial cooperation and technical support they offered along the way of my Ph.D. journey. This work would not have been possible without the financial support of the Marie Curie grant from the European Commission in the framework of the REVAMMAD ITN (Initial Training Research network), project number 316990. I would also like to thank REVAMMAD group for the fabulous scientific suggestions I have received on my work during a series of training workshops. Last but not least, I would like to thank my friends and family who offered endless support during my Ph.D. adventure.

Beijing, China, 25.08.2019